CORE
Metadata, citation and similar papers at core.ac.uk
Provided by IntechOpen

We are IntechOpen, the world's leading publisher of Open Access books Built by scientists, for scientists

4,800
Open access books available

122,000
International authors and editors

135M
Downloads

Our authors are among the

154
Countries delivered to

TOP 1%
most cited scientists

12.2%
Contributors from top 500 universities

WEB OF SCIENCE™

Selection of our books indexed in the Book Citation Index in Web of Science™ Core Collection (BKCI)

Interested in publishing with us?
Contact book.department@intechopen.com

Numbers displayed above are based on latest data collected.
For more information visit www.intechopen.com

7

Resonance Frequency Tracing System for Langevin Type Ultrasonic Transducers

Yutaka Maruyama, Masaya Takasaki
and Takeshi Mizuno
Graduate School of Science &Engineering
Saitama University
Japan

1. Introduction

Ultrasonic vibration is applied to mechatronics fields such as sensor, actuator and so on. In particular, strong ultrasonic vibration is required in the case of applications as actuator. Langevin type ultrasonic transducers have been widely applied to the applications because of the strong vibration. The transducer must be driven at resonance frequency to obtain strong vibration because resonance is utilized in the driving of the transducer. However, the resonance frequency changes depending on environment of usage such as temperature and mechanical load. Note that, in the case of actuators, high-power driving is required; substantial increase of temperature is considered because of large applied voltage to the transducer; and that mechanical load on the actuator continuously changes during the operation. When the frequency of the driving signal differs from the resonance frequency, the vibration amplitude of the transducer reduces dramatically. Therefore, to maintain the strong vibration, the frequency of the driving signal should be tuned according to the change of the resonance frequency - namely, the frequency of the driving signal should trace the resonance frequency.

Vibration feedback oscillator has been widely used for the trace. In the oscillator, motional voltage that is proportional to the vibration velocity of the transducer is positively fed back to the power amplification section of the oscillator. However, the amplitude of the oscillating signal fluctuates depending on the change of the mechanical load. To solve the fluctuation problem, constant velocity controlled motional feedback oscillator was proposed (Ide, 1968; Si & Ide, 1995). In this system, the gain of the power amplification section relates to the response performance of the trace. Therefore, both the gain and the response performance cannot be arbitrarily selected. In addition, this oscillator needs a velocity sensor to obtain the motional voltage. On the other hand, tracing systems using voltage-controlled oscillator (VCO) were proposed (Shimizu & Saito, 1978). In these systems, the gain of the amplifier does not relate to the response performance of the trace since the frequency is directly controlled. Additionally, the systems do not need the velocity sensor. The frequency of the oscillating signal is controlled in the VCO according to the phase or absolute value of admittance of the transducer that changes with the resonance frequency.

In particular, the system utilizing admittance phase is based on the phase-locked loop (PLL) and marked well trace performance. Advanced analyses and experiments about the PLL-based tracing system were curried out to enhance the trace performance of the system (Hayashi, 1991; Hayashi, 1992). However, these systems include a loop filter to obtain a DC signal that is proportional to the admittance phase. The loop filter must be designed specifically for each transducer so as to remain the stability of the closed-loop system.
This paper proposes a resonance frequency tracing system without the loop filter based on digital PLL. This system consists of the microcomputer, detecting circuits and a direct digital synthesizer (DDS). In the system, the admittance phase is obtained as not analog signal but digital data. Therefore, the system does not include the loop filter. The system has also connection with a liquid crystal display (LCD), a host computer and so on as the intelligent function. The proposed system was fabricated. The system configuration and a method to detect the admittance phase are presented.
Ultrasonic dental scalar is introduced as an example of applications of the proposed tracing system. The trace performance of the proposed system is evaluated from step response of the oscillating frequency with a transducer mounted in the dental scalar. In this application, the proposed tracing system is utilized for dental diagnosis in addition to avoiding amplitude reduction. The diagnosis is based on the stiffness estimation. Stiffness of an object can be estimated from the change of the resonance frequency of a piezoelectric transducer caused by contact with the object (Aoyagi & Yoshida, 2006). The proposed system can estimate the stiffness of teeth because the system obtains the resonance frequency of the transducer in real time. Trials of stiffness estimation using the proposed system are reported.

2. Langevin Type Ultrasonic Transducer

Figure 1 shows an example structure of Langevin type ultrasonic transducers. The transducer consists of metal blocks, PZT elements and electrodes. The PZT elements and the electrodes are bolt clamped by the metal blocks. When the alternative voltage is applied to the electrodes, longitudinal vibration is generated. Larger vibration amplitude can be observed at the resonance frequency. In the case of resonance at longitudinal first-order mode, vibration loops and a node are located at the both ends and the middle of the transducer, respectively. For some application, one of the two metal blocks is shaped into a hone, as illustrated in the figure, to enhance the mechanical vibration amplitude.
Characteristics of a sample transducer shaped like the example was investigated. Frequency responses of vibration amplitude were measured with the change of applied voltage. The vibration on the top of the hone was measured by a laser Doppler vibrometer. The measurement results are shown in Fig. 2 with admittance phase (phase difference between the exciting current and the applied voltage). Each curve about mechanical vibration has a

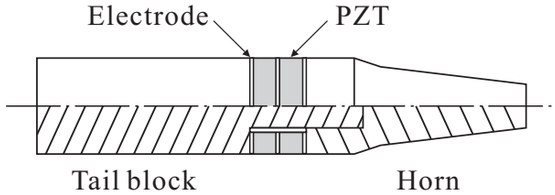

Fig. 1. Example structure of Langevin type ultrasonic transducers.

local peak. The frequency on the peak means resonance frequency. These results demonstrate that resonance frequency shifts to lower frequency region according to the increase of the applied voltage. On the other hand, admittance phase meets a certain value (around 0 [deg]) at resonance frequencies.
Vibration amplitude was measured while the top of the hone was contacted with an object.

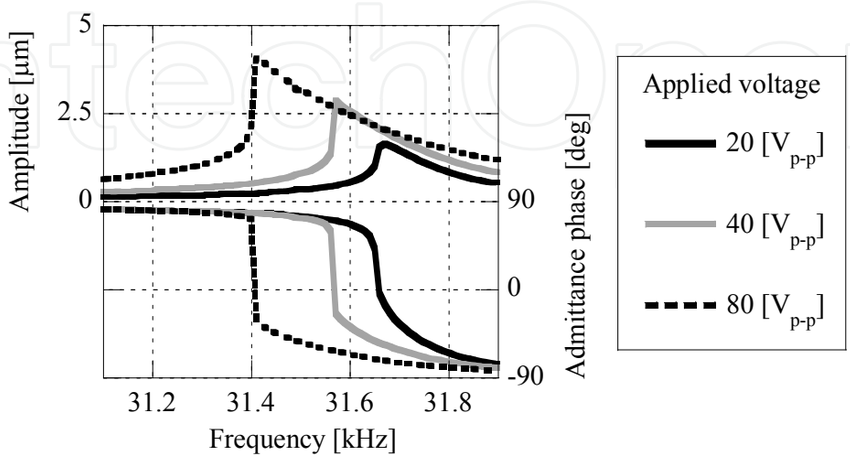

Fig. 2. Frequency responses of vibration amplitude on the front edge and admittance phase of the transducer with the changing amplitude of applied voltage at a condition of no load.

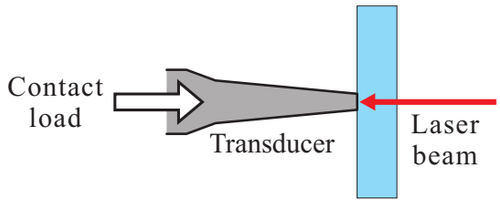

Fig. 3. Vibration amplitude measurement with contacting an object.

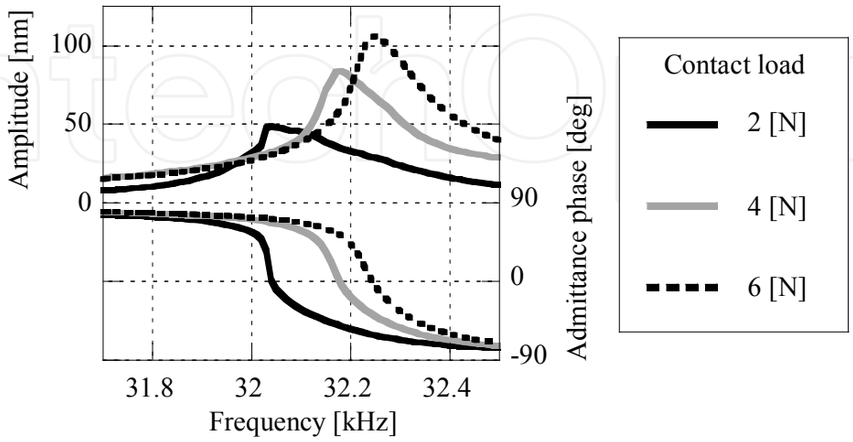

Fig. 4. Frequency responses of vibration amplitude in the front edge and current phase of the transducer with the changing contact load.

The transducer was vertically contacted with a transparent object (an acrylic resin) with a contact load. The vibrometer laser beam was irradiated through the resin, as shown in Fig. 3. Through the measurement, operating frequency was swept with constant amplitude of driving voltage. Frequency responses of the vibration amplitude with the change of contact load are shown in Fig. 4. Admittance phases are also shown in the figure. Local peaks of the amplitude mean resonance frequencies. It can be seen that resonance frequency shifts to the higher frequency region according to the increase of the contact load. Admittance phase changes dramatically around the resonance and meets a certain value (around 0 [deg]: same as the previous result) at the resonance frequency.

3. Resonance Frequency Tracing System

3.1 Overview

As described in the previous section, resonance frequency of the Langevin type ultrasonic transducer changes according to the various reasons. To keep strong vibration, resonance frequency should be traced during the operation of the transducer. In this research, tracing system based on admittance phase measurement is proposed. A microcomputer was applied for the measurement. Tracing algorithm was also embedded in the computer. Other intelligent functions such as communication with other devices can be installed to the computer. Therefore, this system has extensibility according to functions of the computer. Overview of the fabricated resonance frequency tracing system is shown in Fig. 5. The system consists of a computer unit, an amplifier, voltage/current detecting circuit and a wave forming circuit. The computer unit includes a microcomputer (SH-7045F), a DDS and a COM port. The computer is connected to a LCD, a PS/2 keyboard and an EEPROM to execute intelligent functions.

3.2 Oscillating unit

To oscillate driving voltage, sinusoidal wave, the DDS is used. The synthesizer outputs digital wave amplitude data directly at a certain interval, which is much shorter than the cycle of the sinusoidal wave. The digital data is converted to analog signal by an AD converter inside. The frequency of the wave is decided by a parameter stored in the synthesizer. The parameter can be modified by an external device through serial

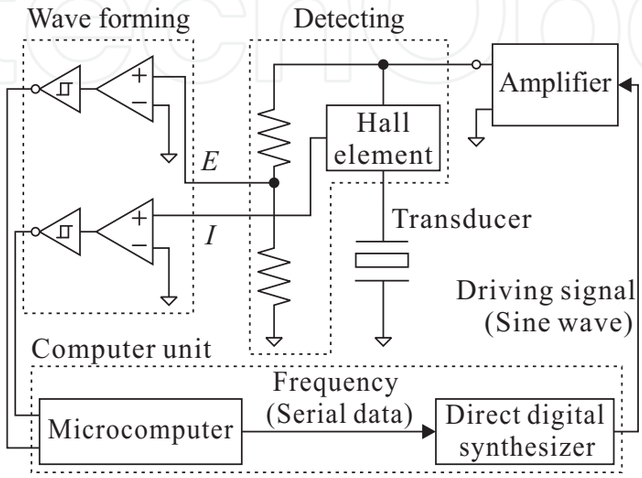

Fig. 5. Overview of resonance frequency tracing system.

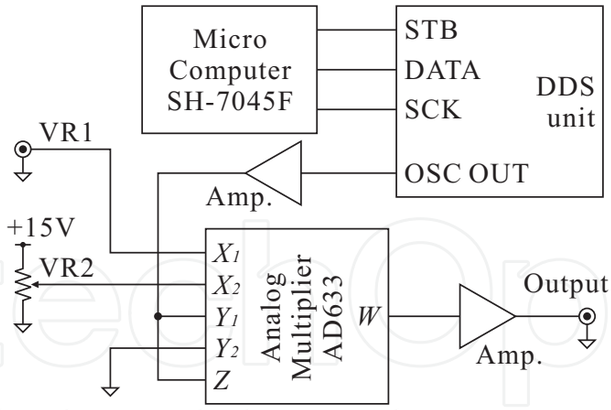

Fig. 6. A direct digital synthesizer and volume control.

communication. In this system, the synthesizer is connected to the microcomputer through three wires, as shown in Fig. 6. The DDS unit includes the AD converter and a LPF. Voltage of the generated sinusoidal wave is amplified and arranged by an analog multiplier (AD633). To control the voltage, the unit has an external DC input VR1 and a volume VR2. Multiplying result W is described as

$$W = \frac{(X_1 - X_2)}{10}(Y_1 - Y_2) + Z \,. \tag{1}$$

The result is amplified. Arranging the DC voltage of VR1 and VR2, the amplitude of the oscillated sinusoidal wave can be controlled continuously.

3.3 Detecting unit

To measure phase difference between applied voltage and current, amplified driving voltage is supplied to the ultrasonic transducer through a detecting unit illustrated in Fig. 7. The applied voltage is divided by a variable resistance, filtered and transformed in to rectangular wave by a comparator. The comparative result is transformed into TTL level pulses. The current flowing to the transducer is detected by a hall element. Output signal from the element is filtered and transformed in the same manner as the voltage detecting. Phase difference of these pulse trains is counted by the microcomputer. To monitor amplitude of the voltage and the current, half-wave rectification circuits and smoothing circuits are installed in the unit. AD converters of the microcomputer sample voltages of the output signals.

3.4 Control unit

A control unit comprises the microcomputer, a keyboard, a LCD, a COM port and an EEPROM, as described in Fig. 8. Commands to control the computer can be typed using the keyboard. Status of the system is displayed on the LCD. A target program executed in the computer is written through the COM port. Control parameters can be stored in the EEPROM. The system has such intelligent functions. The pulses transformed in the detecting unit are input to a multifunction timer unit (MTU) of the microcomputer. T_c (the

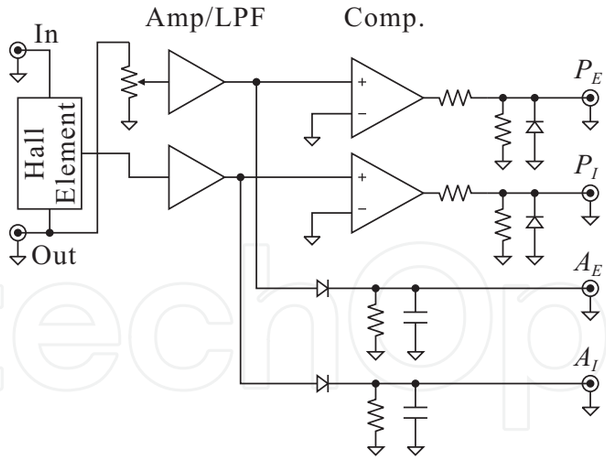

Fig. 7. Voltage/current detecting unit.

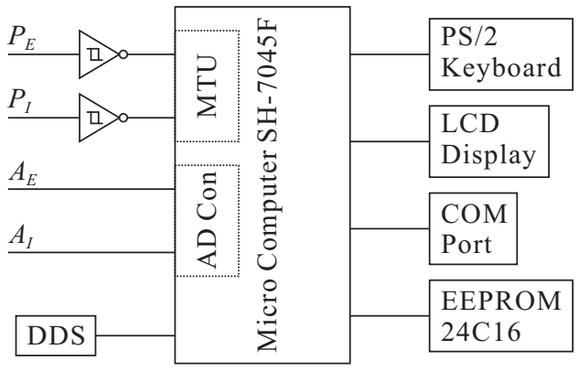

Fig. 8. Control unit with a microcomputer.

time between rising edges of P_E) and T_I (the time between rising edge of P_E and trailing edge of P_I) are measured by the unit, as shown in Fig. 10. The phase difference is calculated from

$$\varphi = 180 \times \frac{T_C - 2T_I}{T_C}. \tag{2}$$

This value is measured as average in averaging factor N_a cycles of pulse signal P_E. Thus, the operating frequency is updated every N_a cycles of the driving signals. The updated operating frequency f_{n+1} is given by

$$f_{n+1} = f_n - K_p(\phi_r - \phi), \tag{3}$$

where f_n is the operating frequency before update, ϕ_r is the admittance phase at resonance, ϕ is the calculated admittance phase from eq. (2) (at a frequency of f_n), K_p is a proportional feedback gain. To stabilize the tracing, K_p should be selected as following inequality is satisfied.

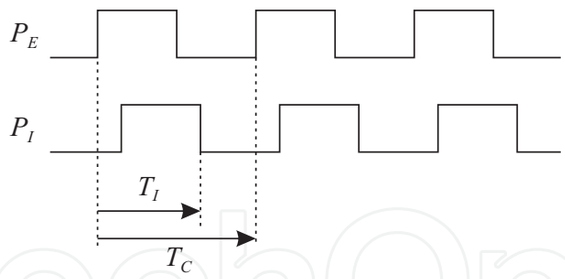

Fig. 9. Measurement of cycle and phase diference.

$$K_p < \frac{2}{S}, \tag{4}$$

where S is the slope of the admittance phase vs. frequency curve at resonanse frequency. The updated frequency is transmitted to the DDS. Repeating this routine, the operating frequency can approach resonance frequency of transducer.

4. Application for Ultrasonic Dental Scaler

4.1 Ultrasonic dental scaler

Ultrasonic dental scaler is an equipment to remove dental calculi from teeth. the scaler consists of a hand piece as shown in Fig. 10 and a driver circuit to excite vibration. A Langevin type ultrasonic transducer is mounted in the hand piece. the structure of the transducer is shown in Fig. 11. Piezoelectric elements are clamped by a tail block and a hone block. A tip is attached on the top of the horn. The blocks and the tip are made of stainless steel. The transducer vibrates longitudinally at first-order resonance frequency. One vibration node is located in the middle. To support the node, the transducer is bound by a silicon rubber.

To carry out the following experiments, a sample scaler was fabricated.Frequency response of the electric charactorristics of the transducer was observed with no mechanical load and input voltage of 20 $V_{p\text{-}p}$. The result is shown in Fig. 12. From this result, the resonance

Fig. 10. Example of ultrasonic dental scalar hand piece.

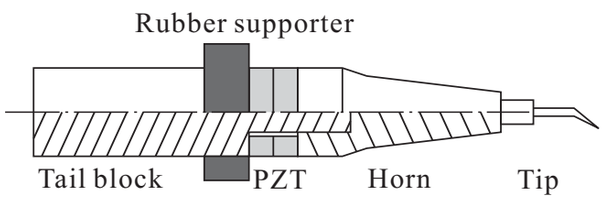

Fig. 11. Structure of transducer for ultrasonic dental scalar.

frequency was 31.93 kHz, admittance phase coincided with 0 at the resonance frequency, electorical Q factor was 330 and the admittance phase response had a slope of -1 [deg/Hz] in the neighborhood of the resonanse frequency.

4.2 Tracing test

Dental calculi are removed by contact with the tip. The applied voltage is adjusted according to condition of the calculi. Temparature rises due to high applied voltage. Therefore, during the operation, the resonance frequency of the transducer is shifted with the changes of contact condition, temperature and amplitude of applied voltage. The oscillating frequency was fixed in the conventional driving circuit. Consequently, vibration amplitude was reduced due to the shift. The resonance frequency tracing system was apllied to the ultrasonic dental scaler.

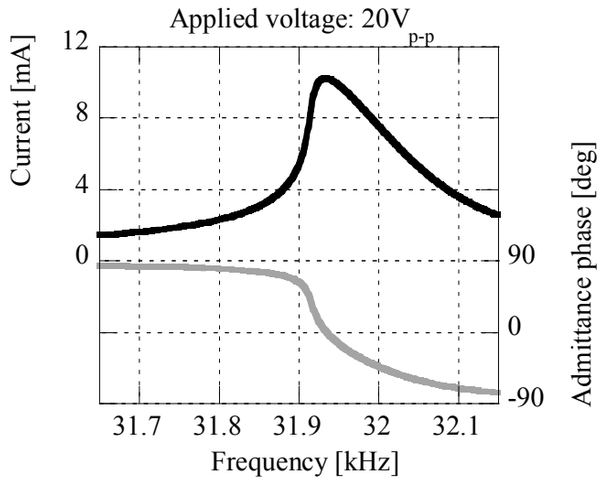

Fig. 12. Electric frequency response of the transducer for ultrasonic dental scalar.

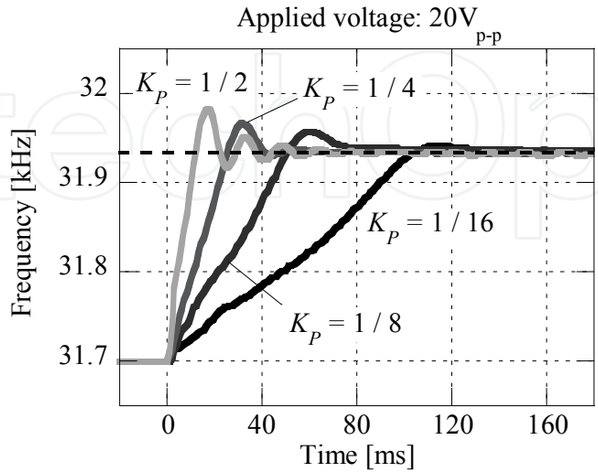

Fig. 13. Step responses of the resonance frequency tracing system with the transducer for ultrasonic dental scaler.

The transducer was driven by the tracing system, where averaging factor N_a was set to 8. To evaluate the system characteristic, step responses of the oscillating frequency were observed in the same condition as the measurement of the electric frequency response. In this measurement, initial operating frequency was 31.70 kHz. the frequency was differed from the resonance frequency (31.93 kHz). At a time of 0 sec, the tracing was started. Namely, the terget frecuency was changed, as a step input, to 31.93 kHz from 31.7 kHz. The transient response of the oscillating frequency was observed. The oscillating frequency was measured by a modulation domain analyzer in real time. Figure 13 shows the measurement results of the responces. With each K_p, the oscillating frequency in steady state was 31.93 kHz. the frequency coincided with the resonance frequency. A settling time was 40 ms with K_p of 1/4. The settling time was evaluated from the time settled within ±2 % of steady state value. The response speed is enough for the application to the dental scaler. Contact load does not change faster than the response speed since the scaler is wielded by human. The temperature and the amplitude of applied voltage also do not change so fast in normal operation.

4.3 Dental diagnosis

When the transducer is contacted with an object, the natural frequency of the transdcer is shifted. A value of the shift depends on stiffness and damping factor of the object (Nishimura et. al, 1994). The contact model can be discribed as shown in Fig. 14. In this model, the natural angular frequency of the transducer with contact is presented as

$$\omega = \sqrt{\frac{1}{m}\left(\frac{AE}{l} + K_C\right) - 2\left(\frac{C_C}{2m}\right)^2}\ , \tag{5}$$

where m is the equivalent mass of the transducer, A is the section area of the transducer, E is the elastic modulus of the material of the transducer, l is the half length of the transducer, K_c is the stiffness of the object and C_c is the damping coefficient of the object. Equation (5) indicates that the combination factor of the damping factor and the stiffness can be estimated from the natural frequency shift. The shift can be observed by the proposed resonance frequency tracing system in real time. If the correlation between the combination factor and the material properties is known, the damping factor or the stiffness of unknown material can be predicted. For known materials, the local stiffness on the contacting point can be estimated if the damping factor is assumed to be constant and known. Geometry also can be evaluated from the estimated stiffness. For a dental health diagnosis, the stiffness

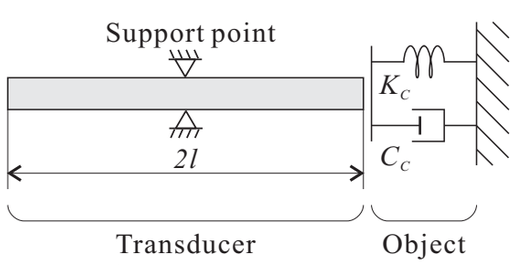

Fig. 14. Contact model of the transducer.

estimation can be applied. To discuss the possibility of the diagnosis, the frequency shifts were measured using the experimental apparatus as shown in Fig. 15. A sample was supported by an aluminum disk through a silicon rubber sheet. The transducer was fed by a z-stage and contacted with the sample. The contact load was measured by load cells under the aluminum disk. This measuring configuration was used in the following experiments.
The combination factor were observed in various materials. The natural frequency shifts in contact with various materials were measured with the change of contact load. The shape and size of the sample was rectangular solid and 20 mm x 20 mm x 5 mm except the $LiNbO_3$ sample. the size of the $LiNbO_3$ sample was 20 mm x 20 mm x 1 mm. The results are plotted in Fig. 16. the natural frequency of the transducer decreased with the increase of contact load in the case of soft material with high damping factor such as rubber. The natural frequency did not change so much in the case of silicon rubber. The natural frequency increased in the case of other materials. Comparing steel (SS400) and aluminum, stiffness of steel is higher than that of aluminum. Frequency shift of $LiNbO_3$ is larger than that of steel

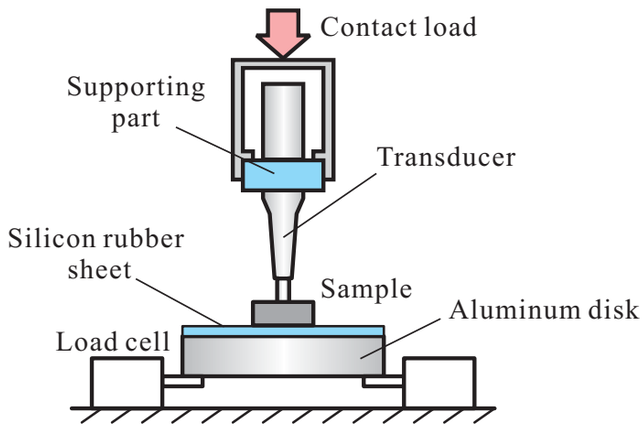

Fig. 15. Experimental apparatus for measurement of the frequency shifts with contact.

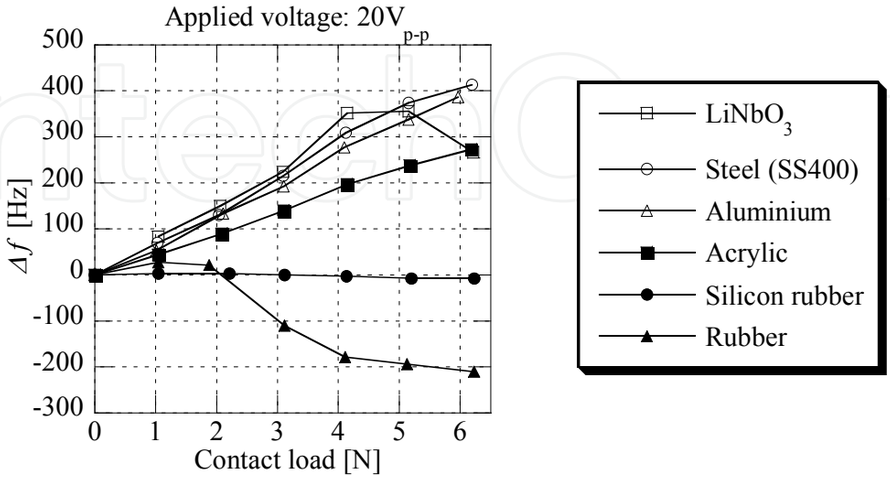

Fig. 16. Measurement of natural frequency shifts with the change of contact load in contact with various materials.

within 4 N though stiffness of $LiNbO_3$ is approximately same as that of steel. This means that mechanical Q factor of $LiNbO_3$ is higher than that of steel, namely, damping factor of $LiNbO_3$ is lower. Frequency shift of $LiNbO_3$ was saturated above 5 N. The reason can be considered that effect of the silicon rubber sheet appeared in the measuring result due to enough acoustic connection between the transducer and the $LiNbO_3$.

The geometry was evaluated from local stiffness. The frequency shifts in contact with aluminum blocks were measured with the change of contact load. The sample of the aluminum block is shown in Fig. 17 (a). Three samples were used in the following experiments. One of the samples had no hole, another had thickness t = 5 mm and the other had the thickness t = 1 mm. Measured frequency shifts are shown in Fig. 17 (b). The frequency shifts tended to be small with decrease of thickness t. These results show that the

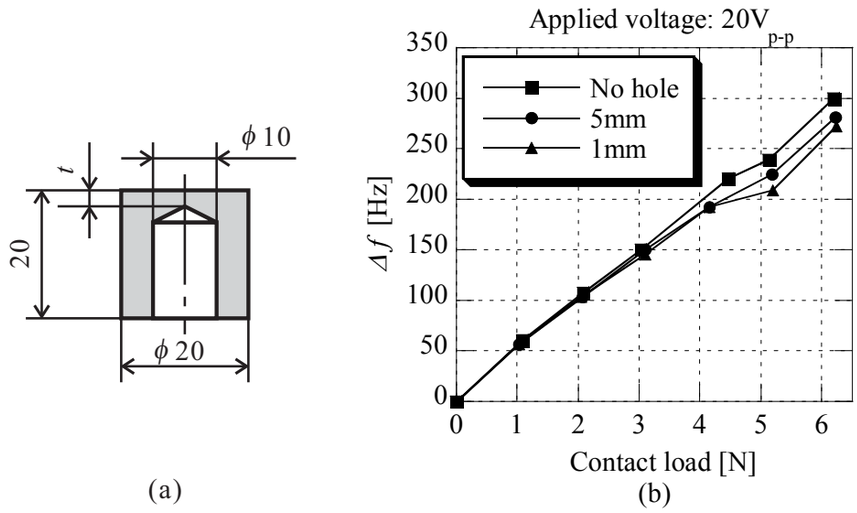

Fig. 17. Measurement of natural frequency shifts with the change of contact load in contact with aluminum blocks.

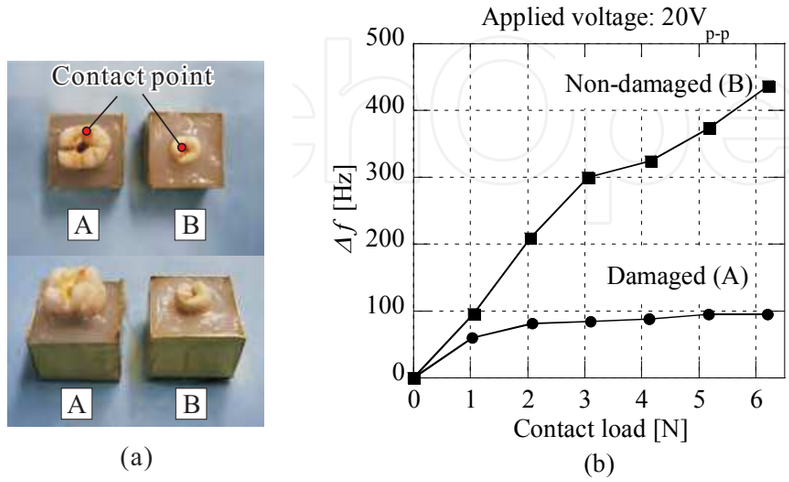

Fig. 18. Measurement of natural frequency shifts with the change of contact load in contact with teeth.

hollow in the contacted object can be investigated from the frequency shift even though there is no difference in outward aspect.
Such elastic parameters estimation and the hollow investigation were applied for diagnosis of dental health. The natural frequency shifts in contact with real teeth were also measured on trial. Figure 18 (a) shows the teeth samples. Sample A is damaged by dental caries and B is not damaged. The plotted points in the picture indicate contact points. To simulate real environment, the teeth were supported by silicon rubber. Measured frequency shifts are shown in Fig. 18 (b). It can be seen that the natural frequency shift of the damaged tooth is smaller than that of healthy tooth.
Difference of resonance frequency shifts was observed. To conclude the possibility of dental health diagnosis, a large number of experimental results were required. Collecting such scientific date is our future work.

5. Conclusions

A resonance frequency tracing system for Langevin type ultrasonic transducers was built up. The system configuration and the method of tracing were presented. The system does not included a loop filter. This point provided easiness in the contoller design and availability for various transducers.
The system was applied to an ultrasonic dental scaler. The traceability of the system with a transducer for the scaler was evaluated from step responses of the oscillating frequency. The settling time was 40 ms. Natural frequency shifts under tip contact with various object, materials and geometries were observed. The shift measurement was applied to diagnosis of dental health. Possibility of the diagnosis was shown.

6. References

Ide, M. (1968). Design and Analysis of Ultorasonic Wave Constant Velocity Control Oscillator, *Journal of the Institute of Electrical Engineers of Japan,* Vol.88-11, No.962, pp.2080-2088.

Si, F. & Ide, M. (1995). Measurement on Specium Acousitic Impedamce in Ultrsonic Plastic Welding, *Japanese Journal of applied physics,* Vol.34, No.5B, pp.2740-2744.

Shimizu, H., Saito, S. (1978). Methods for Automatically Tracking the Transducer Resonance by Rectified-Voltage Feedback to VCO, *IEICE Technical Report*, Vol.US78, No.173, pp.7-13.

Hayashi, S. (1991). On the tracking of resonance and antiresonance of a piezoelectric resonator, *IEEE Transactions on. Ultrasonic, Ferroelectrics and Frequency Control,* Vol.38, No.3, pp.231-236.

Hayashi, S. (1992). On the tracking of resonance and antiresonance of a piezoelectric resonator. II. Accurate models of the phase locked loop, *IEEE Transactions on. Ultrasonic, Ferroelectrics and Frequency Control,* Vol.39, No.6, pp.787-790.

Aoyagi, R. & Yoshida, T. (2005), Unified Analysis of Frequency Equations of an Ultrasonic Vibrator for the Elastic Sensor, *Ultrasonic Technology*, Vol.17, No.1, pp. 27-32.

Nishimura, K. et al., (1994), Directional Dependency of Sensitivity of Vibrating Touch sensor, Proceedings of Japan Society of Precision Engineering Spring Conference, pp. 765-766.

Mechatronic Systems Simulation Modeling and Control

Edited by Annalisa Milella Donato Di Paola and Grazia Cicirelli

ISBN 978-953-307-041-4
Hard cover, 298 pages
Publisher InTech
Published online 01, March, 2010
Published in print edition March, 2010

This book collects fifteen relevant papers in the field of mechatronic systems. Mechatronics, the synergistic blend of mechanics, electronics, and computer science, integrates the best design practices with the most advanced technologies to realize high-quality products, guaranteeing at the same time a substantial reduction in development time and cost. Topics covered in this book include simulation, modelling and control of electromechanical machines, machine components, and mechatronic vehicles. New software tools, integrated development environments, and systematic design methods are also introduced. The editors are extremely grateful to all the authors for their valuable contributions. The book begins with eight chapters related to modelling and control of electromechanical machines and machine components. Chapter 9 presents a nonlinear model for the control of a three-DOF helicopter. A helicopter model and a control method of the model are also presented and validated experimentally in Chapter 10. Chapter 11 introduces a planar laboratory testbed for the simulation of autonomous proximity manoeuvres of a uniquely control actuator configured spacecraft. Integrated methods of simulation and Real-Time control aiming at improving the efficiency of an iterative design process of control systems are presented in Chapter 12. Reliability analysis methods for an embedded Open Source Software (OSS) are discussed in Chapter 13. A new specification technique for the conceptual design of self-optimizing mechatronic systems is presented in Chapter 14. Chapter 15 provides a general overview of design specificities including mechanical and control considerations for micro-mechatronic structures. It also presents an example of a new optimal synthesis method to design topology and associated robust control methodologies for monolithic compliant microstructures.

How to reference

In order to correctly reference this scholarly work, feel free to copy and paste the following:

Yutaka Maruyama, Masaya Takasaki and Takeshi Mizuno (2010). Resonance Frequency Tracing System for Langevin Type Ultrasonic Transducers, Mechatronic Systems Simulation Modeling and Control, Annalisa Milella Donato Di Paola and Grazia Cicirelli (Ed.), ISBN: 978-953-307-041-4, InTech, Available from: http://www.intechopen.com/books/mechatronic-systems-simulation-modeling-and-control/resonance-frequency-tracing-system-for-langevin-type-ultrasonic-transducers

INTECH
open science | open minds

InTech Europe
University Campus STeP Ri

InTech China
Unit 405, Office Block, Hotel Equatorial Shanghai

Slavka Krautzeka 83/A
51000 Rijeka, Croatia
Phone: +385 (51) 770 447
Fax: +385 (51) 686 166
www.intechopen.com

No.65, Yan An Road (West), Shanghai, 200040, China
中国上海市延安西路65号上海国际贵都大饭店办公楼405单元
Phone: +86-21-62489820
Fax: +86-21-62489821

IntechOpen

IntechOpen

© 2010 The Author(s). Licensee IntechOpen. This chapter is distributed under the terms of the Creative Commons Attribution-NonCommercial-ShareAlike-3.0 License, which permits use, distribution and reproduction for non-commercial purposes, provided the original is properly cited and derivative works building on this content are distributed under the same license.

IntechOpen

IntechOpen